
3-1-2022

Water Chemistry, Exposure Routes, and Metal Forms Determine the Bioaccumulation Dynamics of Silver (Ionic and Nanoparticulate) in *Daphnia magna*

Emma Lesser
Smith College

Fatima Noor Sheikh
Smith College

Mithun Sikder
Smith College

Marie Noële Croteau
United States Geological Survey Western Region

Natasha Franklin
United States Geological Survey Western Region

See next page for additional authors

Follow this and additional works at: https://scholarworks.smith.edu/egr_facpubs



Part of the [Engineering Commons](#)

Recommended Citation

Lesser, Emma; Sheikh, Fatima Noor; Sikder, Mithun; Croteau, Marie Noële; Franklin, Natasha; Baalousha, Mohammed; and Ismail, Niveen S., "Water Chemistry, Exposure Routes, and Metal Forms Determine the Bioaccumulation Dynamics of Silver (Ionic and Nanoparticulate) in *Daphnia magna*" (2022). Engineering: Faculty Publications, Smith College, Northampton, MA.
https://scholarworks.smith.edu/egr_facpubs/106

This Article has been accepted for inclusion in Engineering: Faculty Publications by an authorized administrator of Smith ScholarWorks. For more information, please contact scholarworks@smith.edu

Authors

Emma Lesser, Fatima Noor Sheikh, Mithun Sikder, Marie Noële Croteau, Natasha Franklin, Mohammed Baalousha, and Niveen S. Ismail

Water Chemistry, Exposure Routes, and Metal Forms Determine the Bioaccumulation Dynamics of Silver (Ionic and Nanoparticulate) in *Daphnia magna*

Emma Lesser,^{a,1} Fatima Noor Sheikh,^{a,1} Mithun Sikder,^a Marie-Noële Croteau,^b Natasha Franklin,^b Mohammed Baalousha,^c and Niveen S. Ismail^{a,*}

^aPicker Engineering Program, Smith College, Northampton, Massachusetts, USA

^bUS Geological Survey, Menlo Park, California

^cCenter for Environmental Nanoscience and Risk, Arnold School of Public Health, University of South Carolina, Columbia, South Carolina, USA

Abstract: Treatment wetlands utilize various physical and biological processes to reduce levels of organic contaminants, metals, bacteria, and suspended solids. Silver nanoparticles (AgNPs) are one type of contaminant that can enter treatment wetlands and impact the overall treatment efficacy. Grazing by filter-feeding zooplankton, such as *Daphnia magna*, is critical to treatment wetland functioning; but the effects of AgNPs on zooplankton are not fully understood, especially at environmentally relevant concentrations. We characterized the bioaccumulation kinetics of dissolved and nanoparticulate (citrate-coated) ¹⁰⁹Ag in *D. magna* exposed to environmentally relevant ¹⁰⁹Ag concentrations (i.e., 0.2–23 nmol L⁻¹ Ag) using a stable isotope as a tracer of Ag. Both aqueous and nanoparticulate forms of ¹⁰⁹Ag were bioavailable to *D. magna* after exposure. Water chemistry affected ¹⁰⁹Ag influx from ¹⁰⁹AgNP but not from ¹⁰⁹AgNO₃. Silver retention was greater for citrate-coated ¹⁰⁹AgNP than dissolved ¹⁰⁹Ag, indicating a greater potential for bioaccumulation from nanoparticulate Ag. Feeding inhibition was observed at higher dietary ¹⁰⁹Ag concentrations, which could lead to reduced treatment wetland performance. Our results illustrate the importance of using environmentally relevant concentrations and media compositions when predicting Ag bioaccumulation and provide insight into potential effects on filter feeders critical to the function of treatment wetlands. *Environ Toxicol Chem* 2022;41:726–738. © 2021 SETAC

Keywords: Nanoparticles; Biodynamic model; Zooplankton; *Daphnia magna*; Bioavailability; Metal accumulation

INTRODUCTION

Increasing commercial application of engineered nanoparticles (NPs) has led to nearly 2000 nano-enabled products in the consumer market, 20% of which contain silver NPs (AgNPs; Vance et al., 2015). The AgNPs released from these products enter aquatic systems through various pathways, such as stormwater runoff and wastewater effluent (Wiesner et al., 2006). The environmental fate of these particles can vary greatly because of various biological and environmental factors (Dwivedi et al., 2015). Ionic Ag is one of the most toxic metals in aquatic systems (Erickson et al., 1998; Fabrega

et al., 2011). The presence of AgNPs and the potential release of Ag ions can have adverse impacts on aquatic organisms, such as fish, zooplankton, and nematodes, resulting in reduced mobility, impaired reproduction, and mortality (Fabrega et al., 2011). Because stormwater runoff and wastewater effluent can act as sources of AgNP for aquatic systems, it is vital to consider treatment methodologies that remove Ag from water.

Natural treatment systems, such as treatment wetlands, can remove a variety of pollutants including metal-based NPs. For example, sorption, sedimentation, aggregation, and phytoremediation have been widely studied in relation to the removal of AgNPs (Auvinen et al., 2016; Lowry et al., 2012). However, knowledge gaps still exist regarding the fate of AgNPs in relation to filter-feeding organisms. Filter-feeding zooplankton, such as daphnids, are abundant in natural treatment systems; they are a critical link in aquatic food chains and can significantly improve water quality through grazing (Fayer et al., 2000;

This article contains online-only Supporting Information.

¹These authors contributed equally to this work.

* Address correspondence to nismail@smith.edu

Published online 14 December 2021 in Wiley Online Library (wileyonlinelibrary.com).

DOI: 10.1002/etc.5271

Ismail et al., 2019; Jürgens et al., 1997; Shiny et al., 2005; Trout et al., 2002). Adverse effects of AgNPs on daphnids at environmentally relevant conditions could impact the efficacy of treatment wetlands.

Based on predictive models and environmental sampling, expected concentrations of AgNPs in the aquatic environment are estimated to be $<9 \text{ nmol L}^{-1}$ (i.e., $<1 \mu\text{g L}^{-1}$; Gottschalk et al., 2013). Most ecotoxicological studies examining the impact of AgNO_3 and AgNPs on daphnids or other zooplankton use concentrations that are orders of magnitude higher than the expected environmental concentrations (Kwok et al., 2016; Lekamge et al., 2018; Zhao & Wang, 2010). Although high Ag aqueous concentrations are usually required to trigger measurable effects, such as mortality, changes in fecundity, and abnormal swimming (Asghari et al., 2012; Klaine et al., 2008; Newton et al., 2013), these elevated concentrations do not adequately portray bioaccumulation or depict the environmental thresholds at which adverse effects might be expected. The few studies examining the accumulation of Ag in daphnids at lower concentrations show that bioaccumulation of Ag from AgNO_3 and AgNP occurs and that the toxicity of AgNPs can vary orders of magnitude depending on the coating (Allen et al., 2010; Khan et al., 2015; Lam & Wang, 2006). However, these studies do not directly compare waterborne and dieborne uptake of AgNO_3 and AgNP at low concentrations or consider the effects of Ag in complex water matrices, such as wastewater and storm water, which are relevant to natural treatment systems.

In the present study, we characterized waterborne and dietary Ag uptake and elimination kinetics in a model zooplankton species, *Daphnia magna*. We used isotopically enriched Ag, and we synthesized labeled, citrate-coated $^{109}\text{AgNP}$ to trace Ag bioaccumulation dynamics after environmentally realistic exposures. We also conducted experiments using isotopically enriched $^{109}\text{AgNO}_3$ to evaluate and compare the influence of Ag form on bioaccumulation processes. The use of isotopically enriched ^{109}Ag allows for the detection of Ag at environmentally relevant, low concentrations. In addition, we examined the bioaccumulation kinetics of ^{109}Ag ($^{109}\text{AgNP}$ and $^{109}\text{AgNO}_3$) in zooplankton in different water types. Findings from the present study provide insights into the risks of AgNPs in comparison to AgNO_3 to filter-feeding zooplankton under environmentally relevant conditions and help assess the effects of Ag on filter-feeding zooplankton that play a critical role in the operational performance of natural treatment systems.

METHODOLOGY

NP synthesis

Isotopically labeled, citrate-coated $^{109}\text{AgNPs}$ were synthesized by modifying previously published methods (Laycock et al., 2014; Römer et al., 2011; Sikder et al., 2018). Full details of the synthesis procedure are provided in the Supporting Information. All further references to our experimental $^{109}\text{AgNPs}$ refer to citrate-coated $^{109}\text{AgNP}$.

NP characterization

The $^{109}\text{AgNP}$ suspension was characterized using a multi-method approach that included measurements of surface plasmon resonance using ultraviolet–visible spectrometry (UV-vis), core diameter and morphology using transmission electron microscopy (TEM), z-average hydrodynamic diameter (Z-avg), and polydispersity index (PDI) using dynamic light scattering (DLS), zeta potential (ζ) using laser Doppler electrophoresis, and Ag concentrations using inductively coupled plasma mass spectrometry (ICP-MS; Supporting Information, Table S1). The core diameter and morphology of the NPs were determined using a TEM (JEOL USA) operated at 200 keV and equipped with a Jeol EX-230 Silicon Drift Detector (JEOL USA). Sample preparation and analysis for the TEM are described in the Supporting Information. The zeta potential (ζ) was estimated from measurements of electrophoretic mobility of undiluted $^{109}\text{AgNP}$ suspensions using Smoluchowski's approximation. The Z-avg hydrodynamic diameter was calculated from the diffusion coefficient using the Stokes-Einstein equation. Electrophoretic mobility and diffusion coefficient measurements were performed using a Malvern Zetasizer Nano-ZS DLS equipped with an He-Ne 633-nm laser at 25 °C after a 2-min temperature equilibration. Aggregation kinetics of $^{109}\text{AgNPs}$ (4.59 mmol L^{-1}) were measured in triplicate in synthetic moderately hard water (MHW), synthetic stormwater (SW), and secondary treated wastewater (WW; Supporting Information, Tables S2–S4) by monitoring the growth of the Z-avg hydrodynamic diameter as a function of time immediately after mixing with MHW, SW, or WW (more details in the Supporting Information). The UV-vis absorption spectra of the stock suspension of $^{109}\text{AgNPs}$ were collected in the range of 300–600 nm on a Shimadzu 2600 UV-vis instrument (Shimadzu) using a 10-cm path length quartz cuvette.

Organism laboratory culture

Daphnia magna (Connecticut Valley Biological) were maintained in glass aquaria in MHW, SW, and WW (Supporting Information, Tables S2–S4). They were fed ad libitum *Nannochloropsis* sp. green algae (4–6 μm diameter; Florida Aquafarms). *Nannochloropsis* sp. was continuously cultured in sterile ultrapure water (UPW; 18.2 M Ω cm; Thermoscientific Barnstead Nanopure) using Guillard f/2 medium. On the day of the experiment, the appropriate number of adult daphnids (approximately 7 days old, dry wt per daphnid = $0.11 \pm 0.08 \text{ mg}$, $n = 20$) were transferred to experimental beakers containing the experimental solutions spiked with ^{109}Ag (Supporting Information, Tables S2–S4).

Biodynamic model

A bioaccumulation dynamic model (Croteau et al., 2004; Luoma & Rainbow, 2005) was used to characterize ^{109}Ag uptake and elimination in *D. magna* after waterborne and dietary exposures to ^{109}Ag . Variations in ^{109}Ag concentrations in *D. magna* ($[^{109}\text{Ag}]_{\text{org}}$) over time are a function of the

waterborne and dietborne ^{109}Ag uptake as well as ^{109}Ag elimination and body growth dilution (Equation 1).

$$\frac{d[^{109}\text{Ag}]_{\text{org}}}{dt} = k_{\text{uw}} \times [^{109}\text{Ag}]_{\text{water}} + k_{\text{uf}} \times [^{109}\text{Ag}]_{\text{food}} - k_e \times [^{109}\text{Ag}]_{\text{org}} - k_g \times [^{109}\text{Ag}]_{\text{org}} \quad (1)$$

Specifically, ^{109}Ag influx from solution is expressed as a function of k_{uw} (liters per gram per day), a unidirectional ^{109}Ag influx rate constant from solution, and the dissolved or dispersed ^{109}Ag concentration in solution ($[^{109}\text{Ag}]_{\text{water}}$, nanomoles per liter). The k_{uw} value is determined from the slope of the linear relationship between ^{109}Ag uptake rates and ^{109}Ag exposure concentrations. Influx of ^{109}Ag from food varies as a function of k_{uf} (grams per gram per day), a unidirectional ^{109}Ag influx rate constant from food (i.e., algae), and the dietborne metal concentration ($[^{109}\text{Ag}]_{\text{food}}$, nanomoles per gram). The rate constant k_{uf} can be expressed as a function of food ingestion rate (IR, grams per gram per day) and metal assimilation efficiency (AE, unitless; Supporting Information, Equations S2–S5). Changes in $[^{109}\text{Ag}]_{\text{org}}$ are a function of the rate constant of physiological loss (k_e , per day), body growth dilution (k_g , per day), and the metal concentration in *D. magna* ($[^{109}\text{Ag}]_{\text{org}}$, nanomoles per gram). The k_e value is determined using nonlinear regression models (Supporting Information, Equations S6 and S7), and k_g is determined using an exponential growth curve (Supporting Information, Equation S8; Croteau et al., 2011). Calculations are described in Supporting Information, Equations S2–S10.

Membrane transport characteristics

The accumulated ^{109}Ag concentrations in *D. magna* ($[^{109}\text{Ag}]_{\text{org}}$ in nanomoles per gram) can be fitted to a one-site ligand binding model similar to the Michaelis-Mentenequation, which provides insights into the membrane transport processes:

$$[^{109}\text{Ag}]_{\text{org}} = \frac{B_{\text{max}} \times [^{109}\text{Ag}]_{\text{exposure}}}{K_{\text{metal}} + [^{109}\text{Ag}]_{\text{exposure}}} \quad (2)$$

In Equation 2, B_{max} (nanomoles per gram) represents the number of transport sites, K_{metal} (nanomoles per liter) represents the affinity of each transport site, and $[^{109}\text{Ag}]_{\text{exposure}}$ is the ^{109}Ag exposure concentration (nanomoles per liter). The $\log(K)$ value, which is indicative of binding site affinity, is derived from the logarithm of the inverse of K_{metal} (moles per liter).

Waterborne uptake experiments

Silver uptake rates from solution were characterized after ^{109}Ag exposure in MHW, SW, and WW. Silver was added as isotopically enriched $^{109}\text{AgNO}_3$ or $^{109}\text{AgNP}$. The nominal exposure concentrations ranged from 0.2 to 23 nmol L^{-1} ($0.02\text{--}2.5 \mu\text{g L}^{-1}$), covering the range of environmentally relevant concentrations (Nowack et al., 2015). The aqueous ^{109}Ag speciation for the initial dissolved ^{109}Ag concentrations was

calculated using PHREEQC (Parkhurst & Appelo, 2013) for MHW and SW.

For each experiment, adult *D. magna* were collected and transferred into glass beakers filled with 150 ml of media (MHW, WW, or SW) spiked with either $^{109}\text{AgNO}_3$ or $^{109}\text{AgNP}$ to achieve five experimental concentrations and one control. Each exposure concentration had 15 daphnids, resulting in three replicates with five pooled daphnids per replicate. Daphnids were exposed to ^{109}Ag for 2 h. The short exposure allowed for the determination of unidirectional ^{109}Ag influxes while ensuring sufficient ^{109}Ag accumulation for accurate detection. Daphnids were not fed during the exposure period, to minimize fecal scavenging and fecal production. After exposure, daphnids were removed with a pipette and rinsed thoroughly with UPW to remove externally bound ^{109}Ag . *Daphnia magna* were placed on an acid-washed polytetrafluoroethylene (PTFE) sheet (five daphnids, three replicates per treatment). Samples were oven dried at 40°C for 48 h (Model 40 GC; Quincy Lab). Before and after exposure, water samples (2 ml) were taken from each flask after gentle stirring and acidified with concentrated nitric acid (1% final concentration). Separate water samples (4 ml) were taken to determine dissolved ^{109}Ag concentration from AgNPs using ICP-MS following ultrafiltration using 3-kDa Amicon filters. The samples were centrifuged at 4000 rpm for 20 min (Eppendorf 5810R). The reported k_{uw} values for $^{109}\text{AgNP}$ (Equation 1) were corrected to account for the newly dissolved ^{109}Ag from $^{109}\text{AgNPs}$ (Supporting Information, Table S6, and text).

Dietborne uptake experiments

Dietborne uptake experiments were conducted to characterize ^{109}Ag uptake rates after dietary exposures to $^{109}\text{AgNP}$ and $^{109}\text{AgNO}_3$. Algae laden with ^{109}Ag were offered as food to *D. magna*. Algae were labeled to limit surface adsorption, as previously described (Lam & Wang, 2006). A 200-ml suspension of *Nannochloropsis* sp. (concentration of $1 \times 10^6 \text{ cells ml}^{-1}$, algal cell density measured using a Coulter counter; Beckman Coulter Z2) at stationary phase (7 days old) was collected and centrifuged at 2000g and 4°C for 10 min (Eppendorf Centrifuge 5810R). The supernatant was discarded, and the pellet was resuspended in 200 ml of soft water (Supporting Information, Table S5). This step was repeated three times to wash off the growth media. The washed algae were then resuspended in 200 ml of soft water and spiked with different concentrations of ^{109}Ag added as either $^{109}\text{AgNO}_3$ or $^{109}\text{AgNP}$ (i.e., 0.9, 9, and 23 nmol L^{-1}). After a 24-h exposure, algae were centrifuged and resuspended in 25 ml of ethylene diamine tetraacetic acid (5 mM; Thermo Scientific) to remove weakly adsorbed ^{109}Ag (Hassler et al., 2004). Centrifugation and resuspension steps were repeated two times in soft water. The washed spiked algae were resuspended in 5 ml of soft water and used in the experiments. Three replicates of 100 μl of the spiked algal suspension were dried at 40°C for 72 h on pieces of PTFE film and prepared for analysis of ^{109}Ag concentration as described below (see *Sample preparation and analysis*). Experimental

concentrations of algae are shown in Supporting Information, Figure S1. Dissolution of $^{109}\text{AgNP}$ in the presence of algae over the 24-h labeling period was also tested using 3-kDa Amicon ultracentrifuge tubes, as described. This washing procedure was intended to remove weakly sorbed ^{109}Ag . The internalization of Ag by *Nannochloropsis* sp. was not tested, but other studies have shown NP internalization by different algal species (e.g., *Chlamydomonas reinhardtii*; S. Wang et al., 2016; Yan & Wang, 2021).

Daphnids ($n = 100$) were exposed to each dietary ^{109}Ag concentration at an algal cell density of 1×10^4 cells ml^{-1} . After 15 min of feeding, daphnids were collected and rinsed thoroughly (at least three times) with MHW. The short feeding duration was chosen because the gut residence time of food ingested by *D. magna* is less than 1 h (Gillis et al., 2005; Riggler, 1961; Schindler, 1968), thereby avoiding the confounding influence of efflux on uptake. Fifteen daphnids were collected and prepared for Ag analysis (five daphnids pooled per sample and dried at 40 °C, see details in *Sample preparation and analysis* below). The remaining daphnids were transferred into 1-L beakers filled with clean MHW and fed unspiked (unlabeled) algae at a cell density of 1×10^5 cells ml^{-1} . After 3, 6, 12, and 24 h of depuration, 15 daphnids were sampled and prepared for Ag analysis (five daphnids pooled per sample and dried at 40 °C, see details in *Sample preparation and analysis* below). Depuration media and algal food were renewed after each sampling time point. In addition, water samples (2 ml, $n = 3$) were taken before and after each water renewal. The water samples were acidified to reach a final concentration of 1% HNO_3 and stored until analysis.

Elimination experiments

Elimination experiments were conducted to parameterize rate constants of ^{109}Ag loss in tissue (Supporting Information, Equation S7), which were used to quantify and compare the retention of ^{109}Ag accumulated after exposure to either $^{109}\text{AgNO}_3$ or $^{109}\text{AgNP}$. Specifically, 200 *D. magna* were exposed to 0.9 nmol L^{-1} of each form of ^{109}Ag in MHW for 24 h in 1-L beakers. Results from waterborne uptake experiments informed the selection of the exposure concentration to ensure sufficient ^{109}Ag accumulation to allow detection. Daphnids were not fed during the exposure period, to minimize fecal production and scavenging. After exposure, daphnids were collected using a mesh screen, rinsed thoroughly with MHW, and placed into 500 ml of MHW. Fifteen daphnids were sampled after 0, 2, 4, 8, 24, 48, 72, and 120 h of depuration (five daphnids pooled per sample, three replicates, dried at 40 °C). Water and algae were renewed after each sampling. Daphnids were fed unspiked algae at cell counts of 1×10^5 cells ml^{-1} . Before and after renewal, water samples were collected (2 ml, $n = 3$), acidified (1% HNO_3), and stored until analysis.

Sample preparation and analysis

To minimize unintended metal contamination, all labware, vials, and PTFE sheets were soaked for at least 24 h in nitric acid

or nitric acid and hydrochloric acid baths (10%–30%) and rinsed several times with UPW. Dried daphnid and algal samples were weighed using a microbalance (Mettler Toledo XPR206), placed in fluoropolymer vials (Saville), and digested with 200 μl of 16 N HNO_3 (trace metal grade; Fisher Scientific) in a pressure cooker (All American) for 3 h at approximately 125 °C and 18 psi, as previously described (Croteau et al., 2004). Digested samples were diluted with UPW to reach a final concentration of 5% HNO_3 , spiked with an internal standard (to monitor instrument drift and sensitivity), and filtered using 0.45- μm polyvinylidene fluoride syringe filters (Acrodisc). Dogfish liver certified reference material (DOLT-3; National Research Council Canada) and procedural blanks were digested using the same procedure during each analytical run.

Samples were analyzed for ^{107}Ag and ^{109}Ag by ICP-MS (Agilent 7800 or PerkinElmer NexION 300Q). Measured Ag concentrations in the DOLT-3 were consistently within certified values. Standard reference samples from the US Geological Survey (USGS) were run after approximately every 10 samples. Deviations from the standard values were <10%. Method detection limits were 0.05 and 0.06 nmol L^{-1} for ^{107}Ag and ^{109}Ag , respectively.

Calculation of tracer concentration

The accumulated tracer ^{109}Ag concentrations were determined using previously described equations (Croteau et al., 2011) that allow for the tracking of newly accumulated ^{109}Ag from background levels (Supporting Information, Equations S11–S14). Background ^{109}Ag concentrations ($0.018 \pm 0.018 \text{ nmol g}^{-1}$) in tissue were determined using unexposed daphnids ($n = 20$). The total ^{109}Ag concentrations (Supporting Information, Equation S12) were used in the mass-balance calculations for the media samples.

Statistical analysis

Statistical analyses were completed using SPSS (Ver 27; IBM) and Microsoft Excel (Ver 2104; Microsoft). The statistical significance (p value) was set at 0.05. Analysis of variance (ANOVA), analysis of covariance (ANCOVA), the Kruskal-Wallis test, and the Kolmogorov-Smirnov test were utilized to determine differences among treatment groups. Parametric tests, specifically ANOVA and ANCOVA, were used as a more robust alternative to a nonparametric test for linear data. The ANOVA was used to determine if the dry weight of daphnids varied over time. The ANCOVA was performed on log linear efflux data as well as linear uptake of $^{109}\text{AgNO}_3$ versus $^{109}\text{AgNP}$. Otherwise, nonparametric tests were used because of the small sample sizes and nonnormality of the data. The Kruskal-Wallis test was performed to determine differences in retention rates and percent dissolution after 2 h for different water types. The Kolmogorov-Smirnov test was used to compare distributions of retention data for different ^{109}Ag concentrations and $^{109}\text{AgNO}_3$ versus $^{109}\text{AgNP}$. A Shapiro-Wilk test was used to determine the normality of the $^{109}\text{AgNP}$ size distribution. Mean \pm standard deviation (SD) or propagated error values using the SD are presented for experimental data and

calculations. Both SD and propagated error are referred to as SD in the text. Standard errors are reported for metal binding characteristics and biodynamic rate constants. All data needed to evaluate the conclusions are presented in the text, in the Supporting Information, and in the USGS data release (Croteau et al., 2021).

RESULTS AND DISCUSSION

Characterization of NPs in experimental media

The TEM micrograph shows randomly distributed discrete ^{109}Ag NPs without agglomerates when suspended in UPW (Figure 1A). Particles were spherical in shape and exhibited a consistent log-normal size distribution with a single peak (Shapiro-Wilk test for normality, $p > 0.05$; Figure 1B). The number-weighted ^{109}Ag NP core diameter measured by TEM was 8.3 ± 3.3 nm, with approximately 77% of the particles between 5 and 9 nm (Figure 1B). The Z-avg (intensity-weighted) hydrodynamic diameter measured by DLS was 17.5 ± 0.0 nm with a PDI of 0.37 ± 0.00 (Figure 1C). The average core diameter measured by TEM was almost 50% smaller than the Z-avg hydrodynamic diameter determined by DLS. This diameter difference can be attributed to the higher light scattering intensity of the larger particles and the diffuse layer thickness included in the ^{109}Ag NP hydrodynamic diameter (Baalousha & Lead, 2012). The zeta potential of the synthesized citrate-coated ^{109}Ag NPs was -47.1 ± 1.4 mV, reflecting the colloidal stability of the stock suspension (Römer et al., 2011). The total and dissolved ^{109}Ag concentrations of the ^{109}Ag NP stock suspension were 330 ± 28 and

4.1 ± 0.3 mmol L^{-1} , respectively. The citrate-coated ^{109}Ag NP suspension had a single peak plasmon resonance centered on 390 nm (Figure 1D), which is consistent with previously reported values for citrate-coated ^{109}Ag NPs (Sikder et al., 2018). The physicochemical properties are summarized in Supporting Information, Table S1.

The ^{109}Ag NP aggregation was greatest in MHW and minimal in SW and WW (Supporting Information, Figure S3B). The presence of dissolved organic carbon likely enhanced the colloidal stability of ^{109}Ag NP in WW (Afshinnia et al., 2017, 2018), whereas the greater concentration of divalent electrolytes (i.e., Ca^{2+} and Mg^{2+} ; Supporting Information, Tables S2–S4) likely caused the greater ^{109}Ag NP aggregation in MHW than in SW (Baalousha et al., 2013; Supporting Information, text and Figures S2 and S3).

Waterborne ^{109}Ag uptake in MHW

Silver accumulation rates in *D. magna* after waterborne exposures increased linearly with exposure concentrations up to 6.5 nmol L^{-1} for ^{109}Ag added as ^{109}Ag NP and $^{109}\text{AgNO}_3$ (Figure 2A,B). Less than 6% of the ^{109}Ag associated with the ^{109}Ag NP dissolved during the exposure period (Supporting Table S6), indicating that Ag uptake in *D. magna* occurred predominantly from the ^{109}Ag NP. This low AgNP dissolution is in line with that reported in a previously published study where <10% dissolution was observed for similarly sized particles (Misra et al., 2012). All k_{uw} values for ^{109}Ag NP have been corrected to account for the ^{109}Ag NP dissolution (Supporting Information, Table S6 and text).

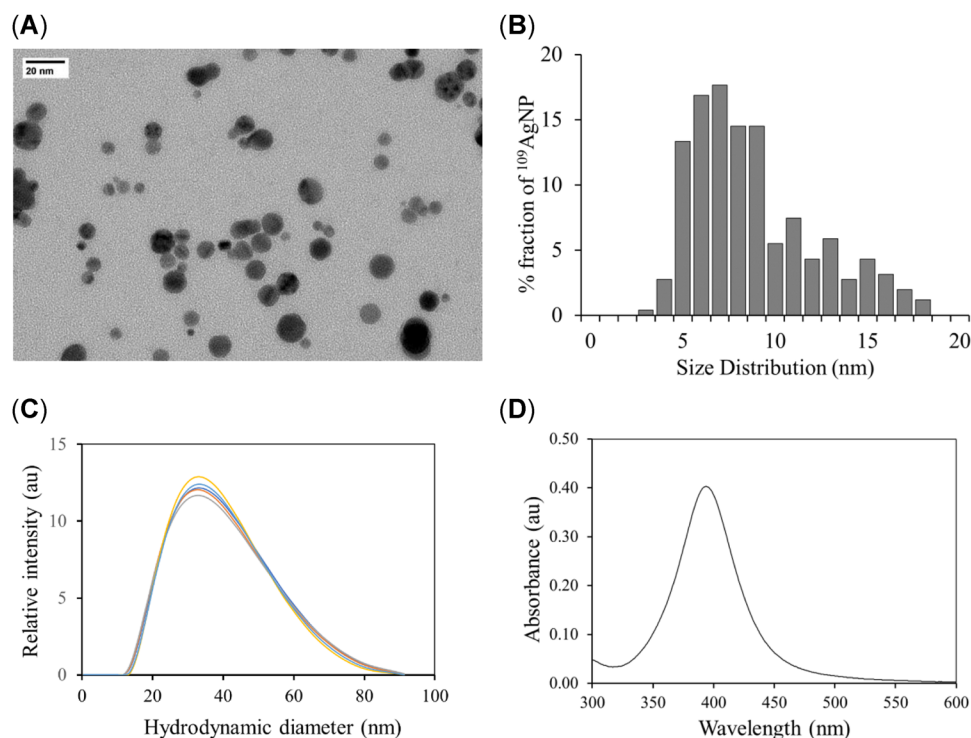


FIGURE 1: Characterization of citrate-coated, isotopically labeled ^{109}Ag NP showing (A) transmission electron microscopy micrograph (scale bar = 20 nm), (B) core diameter distribution ($n = 255$; bin size 1 nm), (C) Z-average hydrodynamic size distributions (five replicates) measured by dynamic light scattering, and (D) visible ultraviolet spectrum showing a plasmon resonance peak at 390 nm. AgNP = silver nanoparticle.

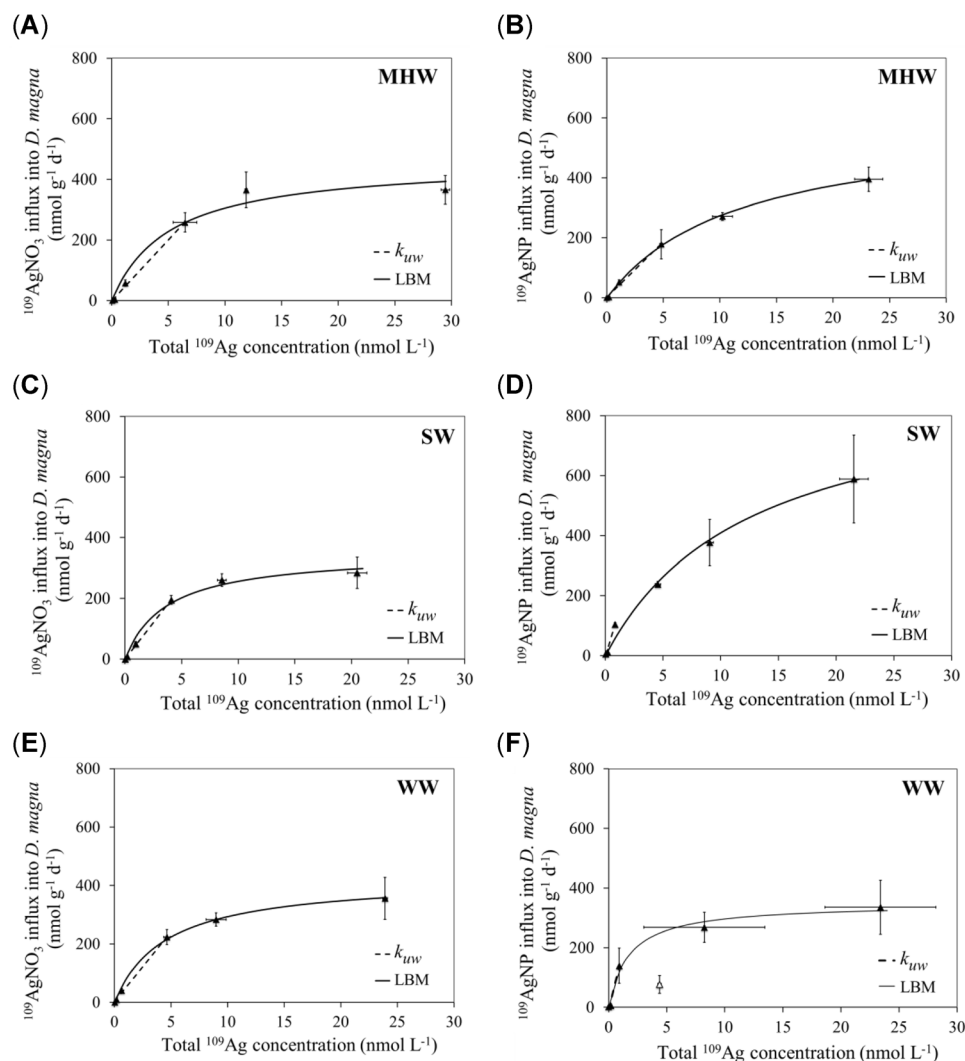


FIGURE 2: Silver (Ag) influx rates (\pm SD) in *Daphnia magna* exposed to ^{109}Ag in experimental media spiked with isotopically labeled $^{109}\text{AgNO}_3$ or citrate-coated, isotopically labeled $^{109}\text{AgNP}$. Water types examined are (A,B) moderately hard water, (C,D) synthetic storm water, and (E,F) secondary treated wastewater. Each data point represents ^{109}Ag concentration for 15 individuals and three water samples (\pm SD). The dashed line represents linear regression relations used to calculate k_{uw} . The solid line represents the nonlinear regression fit to the one-site ligand-binding model. The open symbol in (F) was not included in the model fitting. MHW = moderately hard water; k_{uw} = influx rate constant; LBM = ligand-binding model; AgNP = silver nanoparticle; SW = storm water; WW = wastewater.

As shown in Table 1, the k_{uw} values for both ^{109}Ag forms in MHW (in liters per gram per day) were not significantly different, that is, 40 ± 1 for $^{109}\text{AgNO}_3$ and 37 ± 2 for $^{109}\text{AgNP}$ (ANCOVA, $p > 0.05$; Table 1). The lack of difference suggests that Ag bioavailability is similar between these Ag forms, at least for *D. magna* under the conditions tested. The similarity in k_{uw} between ^{109}Ag forms in MHW suggests a similar uptake mechanism. This finding is different from the previously reported differences in uptake between particulate and dissolved metals. That is, lower bioavailability has often been reported for colloidal-bound metals and metal-based NPs compared to that for dissolved metals (Croteau et al., 2011; Zhao & Wang, 2010). However, this assertion of a similar uptake mechanism for both ^{109}Ag forms in MHW is not supported by the metal binding characteristics. That is (K_{metal}) for $^{109}\text{AgNO}_3$ is half that for $^{109}\text{AgNP}$ (Table 2). Thus, this

difference suggests that waterborne AgNO_3 has a higher site affinity and likely greater toxicity than AgNPs, at least in *D. magna* under the conditions tested. Further studies are required to elucidate this difference.

Previously published studies of Ag bioavailability in *D. magna* reported lower k_{uw} values than those reported in the present study, but these studies used longer exposure times, higher Ag concentrations, or both. Both factors will bias downward the constants that define Ag bioavailability because Ag influxes were not unidirectional (i.e., accumulation rates were influenced by both uptake and elimination processes). Greater exposure concentrations also could yield to accumulation rates obeying second-order kinetics (i.e., ligand-binding kinetics) rather than first-order kinetics (i.e., uptake depends solely on exposure concentrations; Croteau & Luoma, 2007). For example, Khan et al. (2015) exposed *D. magna* for 24 h to

TABLE 1: Biodynamic parameter values (\pm SE) for ^{109}Ag accumulation and elimination by *Daphnia magna* in moderately hard water

Parameter	Symbol (unit)	$^{109}\text{AgNO}_3$	$^{109}\text{AgNP}$
Influx rate constant of ^{109}Ag	k_{uw} ($\text{L g}^{-1} \text{day}^{-1}$)	40 ± 2	37 ± 2
Rate constants of ^{109}Ag loss	k_e (day^{-1})	1.1 ± 0.1	14 ± 4^a 0.14 ± 0.02^b
Ingestion rate	IR ($\text{g g}^{-1} \text{day}^{-1}$)	1.0–20	0.85–13
^{109}Ag assimilation efficiency	AE (%)	57%–62%	16%–43%
Rate constant of dietborne ^{109}Ag	k_{uf} ($\text{g g}^{-1} \text{day}^{-1}$)	0.6–12	0.1–5.8

^aFast exchanging compartment.^bSlow exchanging compartment.

citrate-coated AgNPs (11.6 ± 3.2 nm core particle size, 22.0 ± 1.0 nm hydrodynamic diameter) at concentrations three times higher than those used in the present study ($0\text{--}69$ nmol L^{-1}). Their reported k_{uw} value for AgNP was 40 times lower (i.e., 0.87 ± 0.31 $\text{L g}^{-1} \text{day}^{-1}$) than our value (Khan et al., 2015). Similarly, Lam and Wang (2006) exposed *D. magna* for 8 h to AgNO_3 ($0.07\text{--}8.2$ nmol L^{-1}) and reported a k_{uw} six times lower than our value (i.e., 6.20 ± 0.07 $\text{L g}^{-1} \text{day}^{-1}$). Unidirectional Ag influxes are best captured after short exposures, and the use of stable isotope tracers allows for the detection of Ag uptake at environmentally relevant concentrations even after short exposure durations (Luoma & Rainbow, 2005; W.-X. Wang et al., 1995).

Aggregation of AgNPs at higher concentrations (Afshinnia et al., 2016) could also explain the lower Ag bioavailability reported at higher concentration exposures. Although aggregation occurred in our experiments conducted in MHW (Supporting Information, Figures S2 and S3), it did not trigger detectable differences in ^{109}Ag bioavailability (i.e., similar k_{uw} values were observed for $^{109}\text{AgNPs}$ and dissolved ^{109}Ag ; Table 1). Zhao and Wang (2010) observed a biphasic relationship between Ag uptake in *D. magna* and exposure concentration (i.e., lower bioavailability at lower exposure concentrations and higher bioavailability at higher exposure concentrations). However, the high exposure concentrations used ($20\text{--}4600$ nmol L^{-1} AgNPs), which can influence uptake as well as aggregate size (Afshinnia et al., 2016), impede direct comparisons (Zhao & Wang, 2010).

TABLE 2: Metal binding characteristics and uptake rate constants for ^{109}Ag uptake for *Daphnia magna* exposed for 2 h to a range of isotopically labeled $^{109}\text{AgNO}_3$ and $^{109}\text{AgNP}$ concentrations in different types of water

Water type	^{109}Ag type	k_{uw} (\pm SE; $\text{L g}^{-1} \text{day}^{-1}$) ^a	B_{max} (\pm SE; nmol g^{-1})	K_{metal} (\pm SE; nmol L^{-1})	Log (K) (\pm SE)
Moderately hard water	$^{109}\text{AgNO}_3$	40 ± 2 (4)	460 ± 50	5.1 ± 2.0	8.3 ± 0.2
	$^{109}\text{AgNP}$	37 ± 2 (4)	590 ± 20	12 ± 1	7.9 ± 0.0
Storm water	$^{109}\text{AgNO}_3$	48 ± 1 (4)	350 ± 30	3.7 ± 1.0	8.4 ± 0.1
	$^{109}\text{AgNP}$	130 ± 20 (3)	930 ± 110	13 ± 3	7.9 ± 0.1
Wastewater	$^{109}\text{AgNO}_3$	48 ± 2 (4)	430 ± 20	4.5 ± 0.5	8.3 ± 0.0
	$^{109}\text{AgNP}$	160 ± 30 (3)	350 ± 30^b	1.7 ± 0.6	8.8 ± 0.1

^aNumber of data points included for calculation of k_{uw} is in parentheses.^bThe 4.4 nmol L^{-1} data point was omitted for modeling.Ag = silver; NP = nanoparticle; k_{uw} = influx rate constant; B_{max} = number of transport sites; K_{metal} = affinity of each transport site.

^{109}Ag bioavailability from the aqueous phase in different media

For all three water exposures (MHW, SW, WW) the majority of ^{109}Ag added as $^{109}\text{AgNO}_3$ and $^{109}\text{AgNP}$ remained in suspension (Supporting Information, Tables S6 and S7), and uptake varied based on both the form of ^{109}Ag and the water type. Detailed information on dissolution and uptake can be found in Supporting Information, Tables S6 and S7.

The chemical composition of the exposure media affected ^{109}Ag bioavailability (Table 2 and Figure 2; Supporting Information, Tables S6 and S7). Bioavailability of ^{109}Ag was greater in SW and WW compared to MHW for both ^{109}Ag forms, but the difference was more pronounced for $^{109}\text{AgNP}$ than for $^{109}\text{AgNO}_3$. That is, k_{uw} values for $^{109}\text{AgNP}$ were more than three times greater in SW and WW compared to MHW. The greater ^{109}Ag bioavailability from $^{109}\text{AgNP}$ exposures in SW and WW compared to that in MHW may be due, in part, to the lower AgNP aggregation in these chemically complex media. As shown in Supporting Information, Figures S2 and S3, $^{109}\text{AgNP}$ aggregated almost instantly in MHW compared to the negligible aggregation observed in SW and WW over 10 min. The influence of dissolution on AgNP bioavailability among the media was inconsequential (i.e., dissolution of $^{109}\text{AgNP}$ in MHW, SW, and WW was statistically the same after 2 h; Kruskal-Wallis, $p > 0.05$). The difference in ^{109}Ag bioavailability from $^{109}\text{AgNP}$ exposure among water types highlights the importance of using environmentally relevant water matrices when examining bioavailability and potential toxicity. Data from our experiments show that some ligand-rich water types increase Ag bioavailability from $^{109}\text{AgNP}$ exposures, which can exacerbate toxicity.

Speciation modeling (Supporting Information, Tables S8 and S9) reveals that the dominant form of Ag varies between water types, which has implications for bioavailability and toxicity. In MHW, Ag^+ dominates (91%), whereas in SW, 85% of organo-Ag is expected (namely a glycine Ag complex). Speciation modeling of Ag in WW was impeded by the lack of conditional constants for some of the chemical constituents, but organo-Ag complexes are likely to dominate as predicted for SW. Some organo-Ag complexes could be bioavailable (Luoma et al., 2016). Previous studies have shown that a greater proportion of organo-Ag can increase Ag bioavailability and result in higher binding site densities depending

on the types of organic material present (Bell & Kramer, 2009; Bielmyer et al., 2002; Yang et al., 2014). Although speciation modeling was not completed for WW because of the chemical complexity of this water type, it is likely that WW contains many different forms of organic compounds that can influence bioavailability and modify membrane characteristics. Differences in water chemistry may also affect AgNP behavior. For example, the higher divalent cation concentrations in MHW compared to SW (Supporting Information, Tables S2–S4) are known to be more efficient at destabilizing colloidal suspensions according to the Schulze-Hardy rule (Trefalt et al., 2020), which may cause instability of citrate-coated AgNPs and alter surface charges of AgNPs (Chinnapongse et al., 2011). In addition, natural organic matter (NOM) can adsorb on AgNP surfaces, form NOM coronas, and enhance NP colloidal stability, which in turn increases NP bioavailability (Baalousha et al., 2018; Lynch et al., 2014).

Differences in membrane characteristics could also in part explain the greater bioavailability of ^{109}Ag from $^{109}\text{AgNP}$ exposures in SW and WW compared to that in MHW. However, trends were not evident for both binding site capacities and affinity for $^{109}\text{AgNP}$ treatments (Table 1). On the one hand, binding site capacity (B_{max} ; Equation 2) values varied from 350 to 930 nmol g^{-1} among the different water types: B_{max} was greatest in SW and lowest in WW. The increase in binding site capacity suggests that $^{109}\text{AgNP}$ forms bioavailable ^{109}Ag complexes after binding to either glycine or Suwannee River fulvic acids or both (e.g., Suwannee River humic acid has been shown to enhance uptake of Ag from polyvinylpyrrolidone-coated AgNP (Luoma et al., 2016). On the other hand, site affinities ($\log[K]$, Equation 2) were similar in MHW and SW but almost 1 order of magnitude greater in WW. A greater toxicity for Ag after $^{109}\text{AgNP}$ exposures in WW is likely, which corresponds to the greatest ^{109}Ag bioavailability (k_{lw} of $160 \text{ L g}^{-1} \text{ day}^{-1}$). Note that for the WW treatment with $^{109}\text{AgNP}$, the 4.4 nmol L^{-1} data point was excluded from the saturation kinetics calculations because of a likely experimental error. Binding characteristics were not appreciably different for $^{109}\text{AgNO}_3$ among the different water types.

Dietborne uptake in MHW

Silver accumulation rates in daphnids varied between 163 and $280 \text{ nmol g}^{-1} \text{ day}^{-1}$ when exposed to dietary ^{109}Ag concentrations ranging from 12 to 221 nmol g^{-1} (Figure 3). Correlation between ^{109}Ag influxes and dietary ^{109}Ag concentrations was not apparent for either form of ^{109}Ag (Figure 3A). Dissolution of ^{109}Ag from $^{109}\text{AgNP}$ during the 24-h exposure to algae in soft water was <5%. The fraction of dissolved ^{109}Ag in the algal spike was not determined, but the fraction of newly dissolved ^{109}Ag from the $^{109}\text{AgNP}$ in the water during dietary exposure was <1% (data not shown). Hence, ^{109}Ag uptake from water during dietary exposure was inconsequential.

The ^{109}Ag AE by daphnids after dietary exposures was significantly greater after exposure to algae preexposed to $^{109}\text{AgNO}_3$ compared to $^{109}\text{AgNP}$ (Figure 3B; Kolmogorov-

Smirnov, $p < 0.05$). That is, the ^{109}Ag AE from $^{109}\text{AgNO}_3$ varied between 57% and 62%, whereas the ^{109}Ag AE from $^{109}\text{AgNP}$ varied between 16% and 43%. For $^{109}\text{AgNO}_3$, the ^{109}Ag AE was not dependent on exposure concentration (Figure 4; Kruskal-Wallis, $p > 0.05$), but for $^{109}\text{AgNP}$, the ^{109}Ag AE decreased at higher exposure concentrations (Figure 3B; Kruskal-Wallis, $p < 0.05$). Despite the higher percentage of ^{109}Ag retained after exposures to algae preexposed to $^{109}\text{AgNO}_3$, both forms of ^{109}Ag were rapidly eliminated over the first 3–6 h of depuration (Figure 4).

These results align with previous studies with *D. magna* showing that the Ag AE is independent of concentration for dietborne exposures using AgNO_3 (Lam & Wang, 2006) but

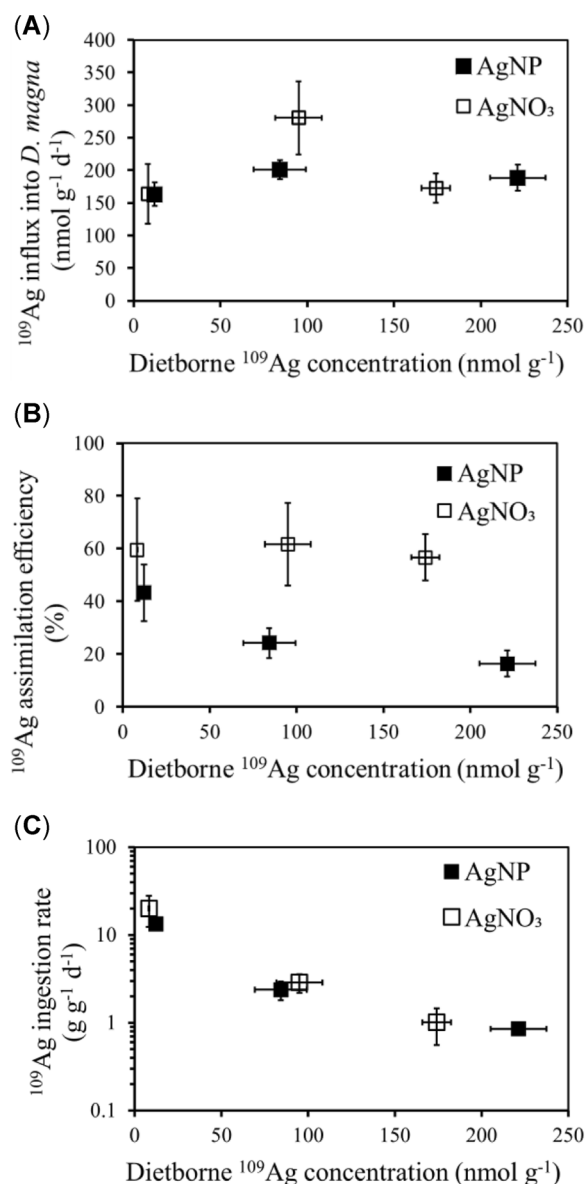


FIGURE 3: (A) Dietborne ^{109}Ag influx ($\pm\text{SD}$), (B) Ag assimilation efficiency ($\pm\text{SD}$), and (C) food ingestion rate ($\pm\text{SD}$) in *Daphnia magna* exposed to a range of dietary concentrations of isotopically labeled $^{109}\text{AgNO}_3$ and citrate-coated $^{109}\text{AgNP}$ concentrations for 15 min. Each data point represents the average value for 15 individuals and three food (algal) samples. AgNP = silver nanoparticle.

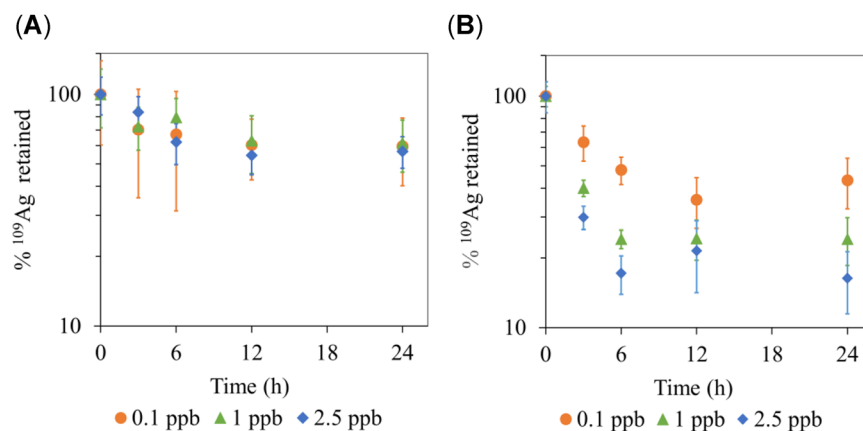


FIGURE 4: Percentage of ^{109}Ag retained (\pm SD) in *Daphnia magna* over time after dietary exposure (15 min) to a range of dietborne concentrations of isotopically labeled (A) $^{109}\text{AgNO}_3$ and (B) citrate-coated $^{109}\text{AgNP}$. Each data point represents the average percent ^{109}Ag retained for 15 individuals. Nominal ^{109}Ag concentrations are listed for each symbol.

decreases with increasing dietary Ag concentrations from AgNP (Zhao & Wang, 2010). It should be noted that the dietary Ag concentrations in these studies were 2–200 times higher than our dietary ^{109}Ag concentrations. The higher dietary Ag concentration could explain the different magnitudes of Ag AEs (Lam & Wang, 2006; Zhao & Wang, 2010). Increasing $^{109}\text{AgNP}$ exposures induce dietary stress at high $^{109}\text{AgNP}$ concentrations, causing a decrease in ^{109}Ag AE. The greater assimilation of ^{109}Ag from dietary $^{109}\text{AgNO}_3$ exposures also suggests a different biological fate and greater risk of toxicity than dietary exposure to $^{109}\text{AgNP}$.

In contrast to the physiological difference in ^{109}Ag assimilation between forms, the behavioral response was similar. That is, the food IR decreased with increasing dietborne ^{109}Ag concentrations after exposure to algae preexposed to either $^{109}\text{AgNO}_3$ or $^{109}\text{AgNP}$ (Table 1 and Figure 3C). The decrease in food IR indicates a shift in feeding behavior in the presence of ^{109}Ag that is independent of the form of ^{109}Ag used. Feeding inhibition and avoidance of food contaminated with Ag have been shown in aquatic organisms including *D. magna* (Croteau et al., 2011; Zhao & Wang, 2010). Previous studies with *Lymnaea stagnalis*, a benthic freshwater snail, showed reduced IRs for cit-AgNP versus ionic Ag at higher metal concentrations, suggesting food avoidance in the presence of AgNP (Croteau et al., 2011). Studies of bivalves with dissolved Ag showed an inverse relationship between AE and IR, resulting in higher AE at lower IR (W.-X. Wang et al., 1995). In the present study, the IR decreased with increasing dietborne concentrations for both forms of ^{109}Ag , whereas the AE only decreased with ^{109}Ag concentration for the $^{109}\text{AgNP}$ exposures. The difference in the effects of dietborne exposure of ionic versus NP-based Ag in *D. magna*, as well as in other freshwater invertebrates previously studied, highlights the complexity of organism responses and effects. The reduced feeding activity due to Ag exposures can trigger adverse effects, which can propagate to higher-level physiological processes like growth and reproduction and ultimately affect the overall population within an aquatic system. The behavioral response of daphnids to a metal-contaminated diet and the impact of contaminated food

on metabolic processes and long-term population health are not well understood and are important areas for future study. In addition, future studies could include the dietary pathway using daphnids in SW and WW to better understand the overall bioaccumulation potential and toxicity risks. A study by Oliver et al. (2014) showed that water chemistry did not impact AgNP dietborne uptake for freshwater aquatic snails, but this relationship may be species-specific and has not been tested with *Daphnia* spp.

Physiological elimination of ^{109}Ag

The longer-term physiological elimination of ^{109}Ag accumulated after waterborne exposures to ^{109}Ag in MHW varied significantly between $^{109}\text{AgNO}_3$ and $^{109}\text{AgNP}$ (ANCOVA, $p < 0.05$), suggesting a different fate of ^{109}Ag within daphnids between ^{109}Ag forms (Figure 5). The ^{109}Ag accumulated after $^{109}\text{AgNO}_3$ exposure was rapidly eliminated during the first 3 days of depuration (Figure 5A). The rate constant of elimination (k_e), estimated using a one-compartment model, was $1.1 \pm 0.1 \text{ day}^{-1}$. Less than 3% of the accumulated ^{109}Ag remained in the daphnid tissues after 3 days of depuration, with no further loss observed afterward. In contrast, elimination of ^{109}Ag accumulated after $^{109}\text{AgNP}$ exposure followed a two-compartment model (Figure 5B), with 30% of the accumulated ^{109}Ag rapidly eliminated during the first 4 h of depuration. After 4 h of depuration, the loss of ^{109}Ag was slower, with a rate constant of loss of $0.14 \pm 0.02 \text{ day}^{-1}$ (Table 1). Body growth dilution did not influence ^{109}Ag elimination (Supporting Information, Equation S8 and Figure S4).

Our data align with previous studies reporting faster efflux and lower retention of accumulated Ag after AgNO₃ compared to AgNP exposures in *D. magna* (Lam & Wang, 2006; Zhao & Wang, 2010). Zhao and Wang (2010) attributed the greater retention of Ag accumulated after AgNP exposure in comparison to AgNO₃ exposure to translocation and biodistribution of AgNP throughout the daphnid body. In addition, the biphasic depuration observed after $^{109}\text{AgNP}$ exposure suggests that fast elimination occurs from particles originating in the gut,

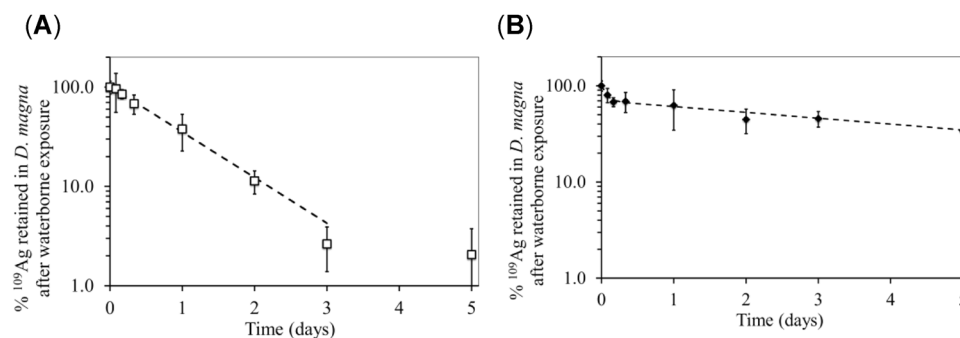


FIGURE 5: Percentage of elimination of ^{109}Ag accumulated after waterborne exposures in moderately hard water to isotopically labeled (A) $^{109}\text{AgNO}_3$ and (B) citrate-coated $^{109}\text{AgNP}$. Each data point represents the average percent ^{109}Ag retained for 15 individuals ($\pm\text{SD}$).

where algae can help force out particles; however, the slow depuration may result from particles distributed in nongut tissues throughout the body (Liu et al., 2019). Hence, increased retention of AgNPs as a result of slow depuration could lead to chronic toxicity for daphnids, having multigenerational effects and ultimately resulting in alterations of overall ecosystem health (Hartmann et al., 2019).

Biodynamic understanding of ^{109}Ag in *D. magna*

We predicted steady-state ^{109}Ag concentration, $[\text{}^{109}\text{Ag}]_{\text{ss}}$, based on waterborne and dietary ^{109}Ag exposure by incorporating the uptake and elimination rate constants derived from our experiments (Supporting Information, Equation S2) along with environmentally relevant concentrations of ^{109}Ag for wastewater-dominated waters, such as treatment wetlands (e.g., 0.009–0.9 nmol L⁻¹; Gottschalk et al., 2013). We assumed that the efflux rate constant, k_e , is similar between exposure routes (Lam & Wang, 2006; Yu & Wang, 2002). Assuming an environmentally relevant chronic exposure of dietary ^{109}Ag from $^{109}\text{AgNO}_3$ and $^{109}\text{AgNP}$ of 10 nmol g⁻¹ and an associated waterborne ^{109}Ag concentration of 1 nmol L⁻¹, model predictions reveal that ^{109}Ag accumulation will be 4.5 times greater for $^{109}\text{AgNP}$ than $^{109}\text{AgNO}_3$. For both forms, ^{109}Ag accumulation will be 1.6–2.8 times greater from food than from water. Specifically, the model predicts an $[\text{}^{109}\text{Ag}]_{\text{ss, diet}}$ of 110 and 410 nmol g⁻¹ for $^{109}\text{AgNO}_3$ and $^{109}\text{AgNP}$, respectively. The $[\text{}^{109}\text{Ag}]_{\text{ss, water}}$ is 38 and 260 nmol L⁻¹ for $^{109}\text{AgNO}_3$ and $^{109}\text{AgNP}$, respectively. The contributions of diet to ^{109}Ag bioaccumulation decrease with increasing ^{109}Ag concentrations for both forms (because of decreases in IR), but higher ^{109}Ag concentrations are less likely to be experienced in natural systems.

Despite seemingly high k_{uw} values, our results show that dietborne ^{109}Ag had a greater influence on body burdens than waterborne ^{109}Ag at environmentally relevant concentrations. In general, filter-feeding species with fast IR, high AE, and low k_e will achieve a higher metal body burden in comparison to species with slower IR, lower AE, and higher k_e (Luoma & Rainbow, 2005). In our study, ^{109}Ag from $^{109}\text{AgNP}$ exposure yielded greater bioaccumulation than $^{109}\text{AgNO}_3$ exposure because of slower elimination rates and greater ^{109}Ag AEs in

D. magna. Dissimilarities in k_e between forms further suggest a different physiological fate of ^{109}Ag between exposures.

Environmental implications

Our results help improve the understanding of the environmental behavior and effects of citrate-coated AgNPs in a model keystone zooplankton species. Zooplankton, such as *D. magna*, play an important role in the functioning of natural treatment systems that can experience continual input of AgNPs. Although continued usage of Ag nanotechnologies may result in increased Ag concentrations in natural waters, the environmental concentrations will likely remain in the low nanomoles per liter range (Gottschalk et al., 2013). Our application of a metal isotope tracer technique and biodynamic modeling allowed the use of environmentally relevant concentrations and the derivation of rate constants required to assess Ag bioavailability among Ag forms, water types, and exposure routes.

We show that AgNPs are bioavailable to daphnids from both water and food. Incorporation of the Ag uptake and loss parameters into the integrated form of Equation 1 (Supporting Information, Equation S2) shows that dietary exposure at lower concentrations, which are likely to be found in natural treatment systems, would result in a high body burden of Ag in *D. magna*. The primary driver for the higher bioaccumulation of ^{109}Ag after $^{109}\text{AgNP}$ exposure compared to $^{109}\text{AgNO}_3$ exposure is the low rate constant of loss. Given the link between bioaccumulation and toxicity, dietborne exposures to Ag (including AgNPs) are likely to elicit adverse effects more readily than waterborne exposure. Because ^{109}Ag from $^{109}\text{AgNPs}$ is efficiently retained in daphnids (Figure 5A), trophic transfer of Ag from AgNPs may be a significant threat to aquatic food chains. Based on the bioavailability and retention of ^{109}Ag from $^{109}\text{AgNPs}$, our results indicate that exposure to AgNPs, which are considered emerging contaminants, could have chronic effects on daphnid populations and subsequent generations. With filter-feeding zooplankton, such as daphnids, playing a crucial role in the overall functioning of natural treatment systems, the effects of Ag exposure in different forms on daphnids and other zooplankton could be fully quantified with further studies.

Future studies could evaluate the longer-term effect of AgNO₃ and AgNPs on the physiological stress in exposed organisms and offspring, growth inhibition, and the potential of overall ecosystem imbalances. In addition, biokinetic and toxicity studies using natural waters and low contaminant concentrations can provide predictions of risk that are more applicable to complex environmental systems such as natural treatment systems.

Supporting Information—The Supporting Information is available on the Wiley Online Library at <https://doi.org/10.1002/etc.5271>.

Acknowledgment—We thank the personnel from the Northampton and Amherst Wastewater Treatment facilities for help collecting wastewater and providing analytical data. We thank the following individuals for project support: M. Anderson from the Center for Aqueous Biogeochemistry at Smith College for ICP-MS support, J. Wopereis from the Center of Microscopy and Imaging at Smith College for TEM support, C. Butler and J. Rodriguez from the University of Massachusetts for access to DLS, and K. Campbell from USGS for speciation modeling using PHREEQC. We thank S. Luoma (USGS emeritus) and M. Diggles (USGS) for constructive feedback on the manuscript. We also thank our two anonymous reviewers for their feedback and insight. This research was supported by a USGS Water Resources Research Center grant (104g: G19AP00006) and Smith College.

Disclaimer—The authors declare that there are no competing interests.

Author Contributions Statement—Investigation, formal analysis, writing–reviewing, and editing: Emma Lesser and Fatima Noor Sheikh. Methodology, investigation, writing–reviewing and editing: Mithun Sikder. Conceptualization and supervision, methodology, investigation, formal analysis, writing–reviewing, and editing: Marie-Noëlle Croteau. Writing–reviewing and editing: Mohammed Baalousha. Methodology, investigation, writing–reviewing and editing: Natasha Franklin. Management of all aspects of the work, including conceptualization and supervision, investigation, interpretation and formal analysis, and writing–original draft, reviewing and editing: Niveen S. Ismail. Emma Lesser and Fatima Noor Sheikh contributed equally to this work.

Data Availability Statement—All data needed to evaluate the findings and conclusions are presented in the article, in the Supporting Information, and in the USGS Science data release (Croteau et al., 2021). Data, associated metadata, and calculation tools are also available from the corresponding author (nismail@smith.edu).

REFERENCES

- Afshinnia, K., Gibson, I., Merrifield, R., & Baalousha, M. (2016). The concentration-dependent aggregation of Ag NPs induced by cystine. *Science of the Total Environment*, 557–558, 395–403. <https://doi.org/10.1016/j.scitotenv.2016.02.212>
- Afshinnia, K., Marrone, B., & Baalousha, M. (2018). Potential impact of natural organic ligands on the colloidal stability of silver nanoparticles. *Science of the Total Environment*, 625, 1518–1526.
- Afshinnia, K., Sikder, M., Cai, B., & Baalousha, M. (2017). Effect of nano-material and media physicochemical properties on Ag NM aggregation kinetics. *Journal of Colloid and Interface Science*, 487, 192–200.
- Allen, H. J., Impellitteri, C. A., Macke, D. A., Heckman, J. L., Poynton, H. C., Lazorchak, J. M., Govindaswamy, S., Roose, D. L., & Nadagouda, M. N. (2010). Effects from filtration, capping agents, and presence/absence of food on the toxicity of silver nanoparticles to *Daphnia magna*. *Environmental Toxicology and Chemistry*, 29(12), 2742–2750. <https://doi.org/10.1002/etc.329>
- Asghari, S., Johari, S. A., Lee, J. H., Kim, Y. S., Jeon, Y. B., Choi, H. J., Moon, M. C., & Yu, I. J. (2012). Toxicity of various silver nanoparticles compared to silver ions in *Daphnia magna*. *Journal of Nanobiotechnology*, 10(1), Article 14. <https://doi.org/10.1186/1477-3155-10-14>
- Auvinen, H., Sepúlveda, V. V., Rousseau, D. P. L., & Du Laing, G. (2016). Substrate- and plant-mediated removal of citrate-coated silver nanoparticles in constructed wetlands. *Environmental Science and Pollution Research International*, 23(21), 21920–21926. <https://doi.org/10.1007/s11356-016-7459-6>
- Baalousha, M., Afshinnia, K., & Guo, L. (2018). Natural organic matter composition determines the molecular nature of silver nanomaterial–NOM corona. *Environmental Science: Nano*, 5(4), 868–881. <https://doi.org/10.1039/C8EN00018B>
- Baalousha, M., & Lead, J. R. (2012). Rationalizing nanomaterial sizes measured by atomic force microscopy, flow field-flow fractionation, and dynamic light scattering: Sample preparation, polydispersity, and particle structure. *Environmental Science & Technology*, 46(11), 6134–6142. <https://doi.org/10.1021/es301167x>
- Baalousha, M., Nur, Y., Römer, I., & Lead, J. R. (2013). Effect of monovalent and divalent cations, anions and fulvic acid on aggregation of citrate-coated silver nanoparticles. *Science of the Total Environment*, 454, 119–131.
- Bell, R. A., & Kramer, J. R. (2009). Structural chemistry and geochemistry of silver–sulfur compounds: Critical review. *Environmental Toxicology and Chemistry*, 18(1), 9–22. <https://doi.org/10.1002/etc.5620180103>
- Bielmyer, G. K., Bell, R. A., & Klaine, S. J. (2002). Effects of ligand-bound silver on *Ceriodaphnia dubia*. *Environmental Toxicology and Chemistry*, 21(10), 2204–2208.
- Chinnapongse, S. L., MacCusprie, R. I., & Hackley, V. A. (2011). Persistence of singly dispersed silver nanoparticles in natural freshwaters, synthetic seawater, and simulated estuarine waters. *Science of the Total Environment*, 409(12), 2443–2450.
- Croteau, M.-N., & Luoma, S. N. (2007). Characterizing dissolved Cu and Cd uptake in terms of the biotic ligand and biodynamics using enriched stable isotopes. *Environmental Science & Technology*, 41(9), 3140–3145.
- Croteau, M.-N., Luoma, S. N., Topping, B. R., & Lopez, C. B. (2004). Stable metal isotopes reveal copper accumulation and loss dynamics in the freshwater bivalve *Corbicula*. *Environmental Science & Technology*, 38(19), 5002–5009. <https://doi.org/10.1021/es049432q>
- Croteau, M.-N., Misra, S. K., Luoma, S. N., & Valsami-Jones, E. (2011). Silver bioaccumulation dynamics in a freshwater invertebrate after aqueous and dietary exposures to nanosized and ionic Ag. *Environmental Science & Technology*, 45(15), 6600–6607. <https://doi.org/10.1021/es200880c>
- Croteau, M.-N., Sikder, M., Ismael, N., Baalousha, M., Lesser, E., Franklin, F., Natasha, N., & Sheikh, F. N. (2021). Data acquired in laboratory experiments conducted with the crustacean *Daphnia magna* to characterize Ag bioaccumulation kinetics after exposures to AgNO₃ or Ag nanoparticles, 2019–2020 [Data set]. US Geological Survey. <https://doi.org/10.5066/P9JPQLUN>
- Dwivedi, A. D., Dubey, S. P., Sillanpää, M., Kwon, Y.-N., Lee, C., & Varma, R. S. (2015). Fate of engineered nanoparticles: Implications in the environment. *Coordination Chemistry Reviews*, 287, 64–78. <https://doi.org/10.1016/j.ccr.2014.12.014>
- Erickson, R. J., Brooke, L. T., Kahl, M. D., Venter, F. V., Harting, S. L., Markee, T. P., & Spehar, R. L. (1998). Effects of laboratory test conditions on the toxicity of silver to aquatic organisms. *Environmental Toxicology and Chemistry*, 17(4), 572–578. <https://doi.org/10.1002/etc.5620170407>
- Fabrega, J., Luoma, S. N., Tyler, C. R., Galloway, T. S., & Lead, J. R. (2011). Silver nanoparticles: Behaviour and effects in the aquatic environment.

- Environmental International*, 37(2), 517–531. <https://doi.org/10.1016/j.envint.2010.10.012>
- Fayer, R., Trout, J. M., Walsh, E., & Cole, R. (2000). Rotifers ingest oocysts of *Cryptosporidium parvum*. *The Journal of Eukaryotic Microbiology*, 47(2), 161–163. <https://doi.org/10.1111/j.1550-7408.2000.tb00026.x>
- Gillis, P. L., Chow-Fraser, P., Ranville, J. F., Ross, P. E., & Wood, C. M. (2005). *Daphnia* need to be gut-cleared too: The effect of exposure to and ingestion of metal-contaminated sediment on the gut-clearance patterns of *D. magna*. *Aquatic Toxicology*, 71(2), 143–154. <https://doi.org/10.1016/j.aquatox.2004.10.016>
- Gottschalk, F., Sun, T., & Nowack, B. (2013). Environmental concentrations of engineered nanomaterials: Review of modeling and analytical studies. *Environmental Pollution*, 181, 287–300. <https://doi.org/10.1016/j.envpol.2013.06.003>
- Hartmann, S., Louch, R., Zeumer, R., Steinhoff, B., Mozhayeva, D., Engelhard, C., Schönherr, H., Schlechtriem, C., & Witte, K. (2019). Comparative multi-generation study on long-term effects of pristine and wastewater-borne silver and titanium dioxide nanoparticles on key life-cycle parameters in *Daphnia magna*. *NanoImpact*, 14, Article 100163. <https://doi.org/10.1016/j.impact.2019.100163>
- Hassler, C. S., Slaveykova, V. I., & Wilkinson, K. J. (2004). Discriminating between intra- and extracellular metals using chemical extractions. *Limnology and Oceanography: Methods*, 2(7), 237–247. <https://doi.org/10.4319/lom.2004.2.237>
- Ismail, N. S., Blokker, B. M., Feeney, T. R., Kohn, R. H., Liu, J., Nelson, V. E., Olive, M. C., Price, S. B. L., & Underdahl, E. J. (2019). Impact of metazooplankton filter feeding on *Escherichia coli* under variable environmental conditions. *Applied and Environmental Microbiology*, 85(23), Article e02006-19. <https://doi.org/10.1128/AEM.02006-19>
- Jürgens, K., Arndt, H., & Zimmermann, H. (1997). Impact of metazoan and protozoan grazers on bacterial biomass distribution in microcosm experiments. *Aquatic Microbial Ecology*, 12, 131–138. <https://doi.org/10.3354/ame012131>
- Khan, F. R., Paul, K. B., Dybowska, A. D., Valsami-Jones, E., Lead, J. R., Stone, V., & Fernandes, T. F. (2015). Accumulation dynamics and acute toxicity of silver nanoparticles to *Daphnia magna* and *Lumbriculus variegatus*: Implications for metal modeling approaches. *Environmental Science & Technology*, 49(7), 4389–4397. <https://doi.org/10.1021/es506124x>
- Klaine, S. J., Alvarez, P. J. J., Batley, G. E., Fernandes, T. F., Handy, R. D., Lyon, D. Y., Mahendra, S., McLaughlin, M. J., & Lead, J. R. (2008). Nanomaterials in the environment: Behavior, fate, bioavailability, and effects. *Environmental Toxicology and Chemistry*, 27(9), 1825–1851. <https://doi.org/10.1897/08-090.1>
- Kwok, K., Dong, W., Marinakos, S., Chilkoti, A., Wiesner, M., Chernick, M., & Hinton, D. (2016). Silver nanoparticle toxicity is related to coating materials and disruption of sodium concentration regulation. *Nanotoxicology*, 10, 1–46. <https://doi.org/10.1080/17435390.2016.1206150>
- Lam, I. K. S., & Wang, W.-X. (2006). Accumulation and elimination of aqueous and dietary silver in *Daphnia magna*. *Chemosphere*, 64(1), 26–35. <https://doi.org/10.1016/j.chemosphere.2005.12.023>
- Laycock, A., Stolpe, B., Römer, I., Dybowska, A., Valsami-Jones, E., Lead, J. R., & Rehkämper, M. (2014). Synthesis and characterization of isotopically labeled silver nanoparticles for tracing studies. *Environmental Science: Nano*, 1(3), 271–283. <https://doi.org/10.1039/C3EN00100H>
- Lekamge, S., Miranda, A. F., Abraham, A., Li, V., Shukla, R., Bansal, V., & Nuggeoda, D. (2018). The toxicity of silver nanoparticles (AgNPs) to three freshwater invertebrates with different life strategies: *Hydra vulgaris*, *Daphnia carinata*, and *Paratya australiensis*. *Frontiers in Environmental Science*, 6, Article 152. <https://doi.org/10.3389/fenvs.2018.00152>
- Liu, Y.-Y., Guo, W.-B., Zhao, Y.-T., Xu, S., Yang, L.-Y., & Miao, A.-J. (2019). Algal foods reduce the uptake of hematite nanoparticles by down-regulating water filtration in *Daphnia magna*. *Environmental Science & Technology*, 53(13), 7803–7811. <https://doi.org/10.1021/acs.est.9b01090>
- Lowry, G. V., Espinasse, B. P., Badireddy, A. R., Richardson, C. J., Reinsch, B. C., Bryant, L. D., Bone, A. J., Deonaraine, A., Chae, S., Therezien, M., Colman, B. P., Hsu-Kim, H., Bernhardt, E. S., Matson, C. W., & Wiesner, M. R. (2012). Long-term transformation and fate of manufactured Ag nanoparticles in a simulated large scale freshwater emergent wetland. *Environmental Science & Technology*, 46(13), 7027–7036. <https://doi.org/10.1021/es204608d>
- Luoma, S. N., & Rainbow, P. S. (2005). Why is metal bioaccumulation so variable? Biodynamics as a unifying concept. *Environmental Science & Technology*, 39(7), 1921–1931. <https://doi.org/10.1021/es048947e>
- Luoma, S. N., Stoiber, T., Croteau, M.-N., Römer, I., Merrifield, R., & Lead, J. R. (2016). Effect of cysteine and humic acids on bioavailability of Ag from Ag nanoparticles to a freshwater snail. *NanoImpact*, 2, 61–69. <https://doi.org/10.1016/j.impact.2016.06.006>
- Lynch, I., Dawson, K. A., Lead, J. R., & Valsami-Jones, E. (2014). Chapter 4—Macromolecular coronas and their importance in nanotoxicology and nanoeotoxicology. In J. R. Lead & E. Valsami-Jones (Eds.), *Frontiers of Nanoscience* (vol. 7, pp. 127–156). Elsevier. <https://doi.org/10.1016/B978-0-08-099408-6.00004-9>
- Misra, S. K., Dybowska, A., Berhanu, D., Luoma, S. N., & Valsami-Jones, E. (2012). The complexity of nanoparticle dissolution and its importance in nanotoxicological studies. *Science of the Total Environment*, 438, 225–232. <https://doi.org/10.1016/j.scitotenv.2012.08.066>
- Newton, K. M., Puppala, H. L., Kitchens, C. L., Colvin, V. L., & Klaine, S. J. (2013). Silver nanoparticle toxicity to *Daphnia magna* is a function of dissolved silver concentration. *Environmental Toxicology and Chemistry*, 32(10), 2356–2364. <https://doi.org/10.1002/etc.2300>
- Nowack, B., Baalousha, M., Bornhöft, N., Chaudhry, Q., Cornelis, G., Cotterill, J., Gondikas, A., Hassellöv, M., Lead, J., Mitrano, D. M., von der Kammer, F., & Wontner-Smith, T. (2015). Progress towards the validation of modeled environmental concentrations of engineered nanomaterials by analytical measurements. *Environmental Science: Nano*, 2(5), 421–428. <https://doi.org/10.1039/C5EN00100E>
- Oliver, A. L.-S., Croteau, M.-N., Römer, I., Lead, J., Stoiber, T., Tejamaya, M., & Luoma, S. N. (2014). Does water chemistry affect the dietary uptake and toxicity of silver nanoparticles by the freshwater snail *Lymnaea stagnalis*? *Environmental Pollution*, 189, 87–91.
- Parkhurst, D., & Appelo, C. (2013). Description of input and examples for PHREEQC version 3: A computer program for speciation, batch-reaction, one-dimensional transport, and inverse geochemical calculations [Techniques and Methods 6–A43]. *US Geological Survey*. <https://doi.org/10.3133/tm6A43>
- Rigler, F. H. (1961). The relation between concentration of food and feeding rate of *Daphnia magna* straus. *Canadian Journal of Zoology*, 39(6), 857–868. <https://doi.org/10.1139/z61-080>
- Römer, I., White, T. A., Baalousha, M., Chipman, K., Viant, M. R., & Lead, J. R. (2011). Aggregation and dispersion of silver nanoparticles in exposure media for aquatic toxicity tests. *Journal of Chromatography A*, 1218(27), 4226–4233. <https://doi.org/10.1016/j.chroma.2011.03.034>
- Schindler, D. W. (1968). Feeding, assimilation and respiration rates of *Daphnia magna* under various environmental conditions and their relation to production estimates. *Journal of Animal Ecology*, 37(2), 369–385. <https://doi.org/10.2307/2954>
- Shiny, K. J., Remani, K. N., Nirmala, E., Jalaja, T. K., & Sasidharan, V. K. (2005). Biotreatment of wastewater using aquatic invertebrates, *Daphnia magna* and *Paramecium caudatum*. *Bioresource Technology*, 96(1), 55–58. <https://doi.org/10.1016/j.biortech.2004.01.008>
- Sikder, M., Lead, J. R., Chandler, G. T., & Baalousha, M. (2018). A rapid approach for measuring silver nanoparticle concentration and dissolution in seawater by UV-vis. *Science of the Total Environment*, 618, 597–607. <https://doi.org/10.1016/j.scitotenv.2017.04.055>
- Trefalt, G., Szilagy, I., & Borkovec, M. (2020). Schulze-Hardy rule revisited. *Colloid and Polymer Science*, 298, 961–967. <https://doi.org/10.1007/s00396-020-04665-w>
- Trout, J. M., Walsh, E. J., & Fayer, R. (2002). Rotifers ingest giardia cysts. *The Journal of Parasitology*, 88(5), 1038–1040. <https://doi.org/10.2307/3285557>
- Vance, M. E., Kuiken, T., Vejerano, E. P., McGinnis, S. P., Hochella, M. F., Jr., Rejeski, D., & Hull, M. S. (2015). Nanotechnology in the real world: Redevolving the nanomaterial consumer products inventory. *Beilstein Journal of Nanotechnology*, 6(1), 1769–1780. <https://doi.org/10.3762/bjnano.6.181>
- Wang, S., Lv, J., Ma, J., & Zhang, S. (2016). Cellular internalization and intracellular biotransformation of silver nanoparticles in *Chlamydomonas reinhardtii*. *Nanotoxicology*, 10(8), 1129–1135. <https://doi.org/10.1080/17435390.2016.1179809>

- Wang, W.-X., Fisher, N. S., & Luoma, S. N. (1995). Assimilation of trace elements ingested by the mussel *Mytilus edulis*: Effects of algal food abundance. *Marine Ecology Progress Series*, 129, Article 165176. <https://doi.org/10.3354/meps129165>
- Wiesner, M. R., Lowry, G. V., Alvarez, P., Dionysiou, D., & Biswas, P. (2006). Assessing the risks of manufactured nanomaterials. *Environmental Science & Technology*, 40(14), 4336–4345. <https://doi.org/10.1021/es062726m>
- Yan, N., & Wang, W.-X. (2021). Novel imaging of silver nanoparticle uptake by a unicellular alga and trophic transfer to *Daphnia magna*. *Environmental Science & Technology*, 55(8), 5143–5151. <https://doi.org/10.1021/acs.est.0c08588>
- Yang, X., Jiang, C., Hsu-Kim, H., Badireddy, A. R., Dykstra, M., Wiesner, M., Hinton, D. E., & Meyer, J. N. (2014). Silver nanoparticle behavior, uptake, and toxicity in *Caenorhabditis elegans*: Effects of natural organic matter. *Environmental Science & Technology*, 48(6), 3486–3495. <https://doi.org/10.1021/es404444n>
- Yu, R.-Q., & Wang, W.-X. (2002). Kinetic uptake of bioavailable cadmium, selenium, and zinc by *Daphnia magna*. *Environmental Toxicology and Chemistry*, 21(11), 2348–2355.
- Zhao, C.-M., & Wang, W.-X. (2010). Biokinetic uptake and efflux of silver nanoparticles in *Daphnia magna*. *Environmental Science & Technology*, 44(19), 7699–7704. <https://doi.org/10.1021/es101484s>